

Phonon Transport in Electronic Devices: From Diffusive to Ballistic Regime

B. Thouy, J.P. Mazellier, J.C. Barbé, G. Le Carval
 LETI-MINATEC
 Commissariat à l'Énergie Atomique (CEA)
 Grenoble, France
 e-mail: jean-charles.barbe@cea.fr

Abstract—This paper presents a Lattice Boltzmann Model applied to phonon transport in silicon-based films, implemented with the OpenLB library [1]. This model is based on the discretization of Boltzmann equation with the “gray” model for phonons. By this approach we can treat heat transfer in complex structures and various materials. We have validated our model by comparing temperature profiles and thermal conductivities in thin films to literature data. Finally, we discuss an improvement of the method in the ballistic case.

Fully Depleted MOSFET, Silicon On Insulator, phonon transport, heat transfer, Lattice Boltzmann Method.

I. INTRODUCTION

In present microelectronics, architectures such as FDSOI transistors (Fully Depleted Silicon On Insulator) illustrated in Figure 1 have been built to improve the electrical performances. Although the insulating BOX fulfills the electrical insulation requirement, it also increases the self-heating of the transistor because of limiting the spreading of phonons to the substrate.

The classical Fourier Model (FM) can not address thermal simulations of such advanced devices since the characteristic lengths are far below the phonon mean free path (mfp~300nm in bulk silicon at 300K). FM does not take into account neither ballistic behaviour of heat transfer at such time and spatial scales nor interactions between high-energy and high-speed phonons (i.e. interactions between optical and acoustic ones). It results in minimizing the temperature elevation in the device [2]. Instead, we should use the Boltzmann-Peierls (BP) equation which describes precisely the transport phenomena [3]. Unlike most of works on this topic, we use a Lattice Boltzmann Method (LBM), a recent fast computational,

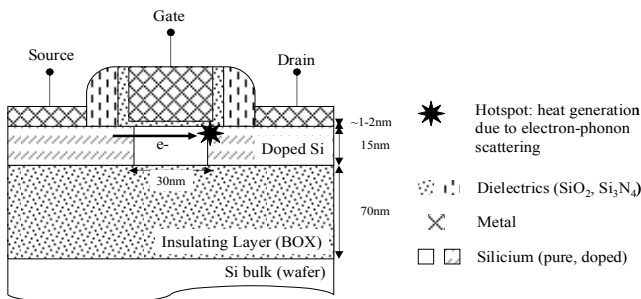


Figure 1 Schematics of the FDSOI device.

multiscale and multidisciplinary method [4].

In this work we present a simple “gray” model on the basis of the LBM. We will demonstrate its validity through a very good agreement with other numerical methods and with experimental data. Then we will propose and discuss the original solution we have developed to address purely ballistic transport.

II. LATTICE BOLTZMANN MODEL

A. Lattice Boltzmann Equation

In the relaxation time approximation, the BP equation can be written as (1):

$$\frac{\partial f}{\partial t} + \vec{c} \cdot \vec{\nabla} f = \frac{1}{\tau} (f^0 - f) + Q_{e-p}, \quad (1)$$

$$f^0 = \frac{1}{e^{\frac{\hbar\omega}{kT}} - 1}, \quad (2)$$

where f is the distribution function of phonons, c the phonon group velocity, τ the mean relaxation time over all interactions between phonons, f^0 the Bose-Einstein equilibrium function (2) and Q_{e-p} the phonon generating rate.

Considering a phonon population with a given frequency and the associated group velocity, taking a constant time step $\delta t \ll \tau$ (I1), the exact solution of (1) at a position \mathbf{x} and at time t is developed in Taylor series at first order in δt [5]:

$$f(\mathbf{x} + \vec{c}\delta t, t + \delta t) - f(\mathbf{x}, t) = \frac{1}{\tau} (f^0(\mathbf{x}, t) - f(\mathbf{x}, t)) + \delta t Q_{e-p}, \quad (3)$$

where $\frac{1}{\bar{\tau}} = \frac{\delta t}{\tau}$ is the normalized relaxation rate. Equation (3) is called the Lattice Boltzmann Equation (LBE) for phonons and is an explicit iterative scheme to solve the native BP equation.

Before explaining the algorithm of the LBM, we show that (3) leads to FM in the diffusive limit, i.e. for Knudsen number Kn below 10^{-2} . Kn is defined as the ratio between the phonon mfp and the feature size of the device. Defining the heat flow and the thermal conductivity as follows:

$$\mathbf{q} = \int_{\Delta\omega} \mathbf{c} \hbar \omega D(\omega) f(\omega) d\omega, \quad (4)$$

$$k = \frac{1}{3} \int_{\Delta\omega} \mathbf{c}^2 \tau \hbar \omega D(\omega) \frac{\partial f^0}{\partial T} \cdot \nabla T \cdot d\omega, \quad (5)$$

where D is the density of states in silicon, \hbar the Planck constant and T the local temperature, we make a multiscale expansion [4] of (3) (for sake of simplicity, phonon generation rate omitted) and thus find:

$$\tau \frac{\partial \mathbf{q}}{\partial t} + \mathbf{q} = -k \cdot \vec{\nabla} T. \quad (6)$$

Equation (6) is the Cattaneo hyperbolic equation for heat transfer, which leads to FM in the steady state.

B. Lattice Boltzmann Model

Now we develop the LB scheme in the ‘‘gray’’ model approximation: the phonon dispersion is taken to be a Debye approximation with constant group velocity whatever the frequency considered.

Keeping the time step δt and the velocity c constant, we also discretize the spatial domain with a regular mesh of lattice step $\delta x = c \cdot \delta t$. In between two neighbouring cells the phonons travel quasi-ballistically because of (11). Into each cell, the propagating directions are discretized and, in 2D, this results in the so-called D2Q8 lattice with 8 propagating directions \mathbf{c}_i (see Figure 2 inset) with corresponding distribution functions f_i ($i=1..8$). Each f_i function is governed by equation (3). The iterative scheme is done in two steps: collision and streaming. The collision step depicting interactions between phonons:

$$f_i(\mathbf{x}, t + \delta t) - f_i(\mathbf{x}, t) = \frac{\delta t}{\tau} (f_i^0(\mathbf{x}, t) - f_i(\mathbf{x}, t)) + \delta t \cdot Q_{e-p,i}. \quad (7)$$

The second step is the streaming step along each propagation direction:

$$f_i(\mathbf{x} + \mathbf{c}_i \cdot \delta t, t + dt) = f_i(\mathbf{x}, t + dt) \quad (8)$$

In Figure 2, we can see that the velocity vectors \mathbf{c}_i have not the same norm, resulting in unphysical anisotropic transport. To recover isotropy, we affect a weight w_i to each direction i : these weights are calculated to respect isotropy relations [4]. For D2Q8, diagonals have a weight of 1/20 and the others directions are weighted by 1/5.

To cover the whole frequency range of phonons, we use energy density e instead of distribution function f_i , defined by:

$$e = \int_{\Delta\omega} \hbar \omega D(\omega) \cdot f(\omega) \cdot d\omega. \quad (9)$$

By integrating (7) using (9), we obtain an analogous LBE for each energy density function e_i :

$$e_i(\mathbf{x} + \mathbf{c}_i \delta t, t + \delta t) - e_i(\mathbf{x}, t) = \frac{1}{\tau} (e_i^0(\mathbf{x}, t) - e_i(\mathbf{x}, t)) + \delta t \cdot Q'_{e-p,i}, \quad (10)$$

where $Q'_{e-p,i}$ is the heat generation power. The relaxation rate $1/\tau$ is an average value over the whole phonon frequency range. e_i^0 is the energy density at thermodynamic equilibrium, given by:

$$e^0 = \sum_{i=1}^D e_i \Leftrightarrow e_i^0 = w_i \cdot e^0. \quad (11)$$

Using the energy conservation principle on (9), the local

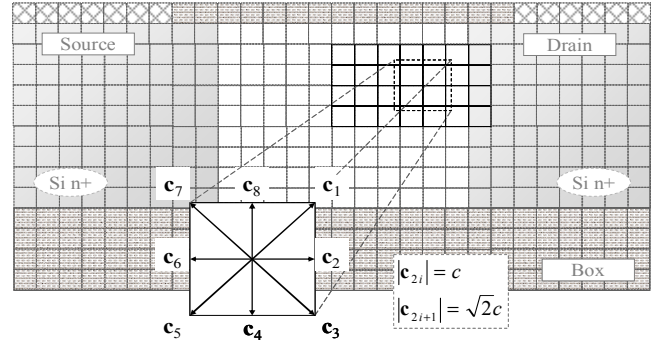


Figure 2 Spatial discretization and D2Q8 lattice. Phonons must travel along these directions.

equivalent temperature can be defined using:

$$e(T) = \int_{\Delta\omega} \frac{\hbar \omega \cdot D(\omega)}{e^{\hbar \omega / kT}} d\omega. \quad (12)$$

C. Boundary conditions

Two different boundary conditions have been implemented. We can either impose a temperature value and then the incoming energy density according to (12). Or we can impose a normal-to-the-surface heat flow: in the ‘‘gray’’ model, from (4) and (9), the heat flow is $\mathbf{q} = c\mathbf{e}$ since the phonon group velocity is constant; hence, the energy density along an incoming direction $i+$ from the opposite outgoing one $i-$ is:

$$e_{i+} = \frac{q_{imp}}{c_i} \cdot \cos(\mathbf{n}, \mathbf{c}_i) + e_{i-}, \quad (13)$$

where \mathbf{n} is the incoming unitary vector normal to the surface.

In addition to these boundary conditions, we have introduced a specularity parameter in order to treat from diffusive to specular boundaries. On a diffusive boundary, outgoing components are isotropically distributed onto all incoming directions, whereas on a specular boundary outgoing ones are reflected on incoming directions with respect to the surface. Finally, we have introduced a transmission parameter to mimic the effects of the interface resistance and thus have a partially transparent partially specular boundary.

Moreover, as we can see on Figure 1, we have to simulate heat transfer in several materials (we do not deal with metals where heat is carried mainly by electrons, not by phonons [3]). The interface is modelled by the theory of Narumanchi [2], where the transmission coefficients are computed by the diffusive mismatch model [6] and discretized according to the LBM. Dealing with two different materials implies two mean group velocities and so two spatial steps. Instead, we choose a non constant time step which complies with both materials properties.

III. RESULTS AND DISCUSSION

After implementation using the OpenLB C++ library [1], we have performed several simulations to validate the model in regard to other equivalent models and experimental data.

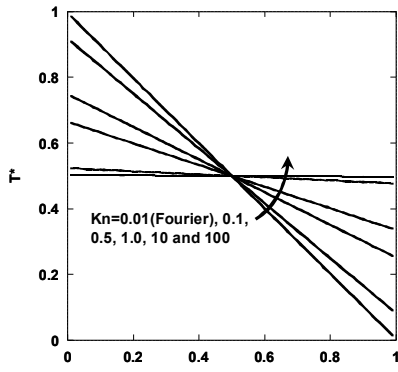


Figure 3 Steady state temperature gradients cross a silicon film for different Kn ; lengths and temperatures are normalized respectively by layer thickness and total temperature variation (1K).

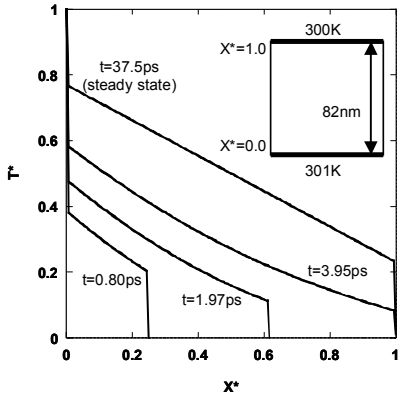


Figure 4 Transient temperature profiles across a 82nm-thick silicon layer with an imposed mfp of 41nm; lengths and temperatures are normalized respectively by the layer thickness and the total imposed temperature variation.

A. LBM temperature profiles

First a planar thin silicon film has been considered. Figure 3 presents the temperature profile across the film for several Kn , from diffusive to ballistic regimes, ($mfp=41nm$). As Kn increases, temperature discontinuities appear at film boundaries and temperature profiles go flat, i.e. the effective thermal conductivity decreases with the film thickness. These results are in very good agreement with other simulations [7][8] and the temperature jumps can be seen as boundary thermal resistances.

We have computed the transient temperature in a quasi-ballistic case ($Kn=0.5$). The whole structure is at 300K and at $t \geq 0$ the temperature on the lower boundary is fixed to 301K. Figure 4 shows instantaneous temperature profiles in the silicon film. Ballistic phenomena appear in temperatures jumps at boundaries; however the inner temperature profile follows a slight parabolic trend like in diffusive regime.

B. Thermal conductivities

Figure 5 presents the evolution of the effective cross plane thermal conductivity versus thickness of the planar silicon film. We have used a constant relaxation time of 6.54ps [2]. This value has been derived carefully from Holland's model [9], averaged over all acoustic modes and taking into account

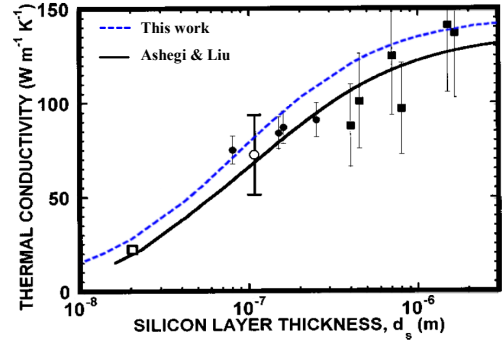


Figure 5 Thermal conductivity dependence with layer thickness. Solid line and original figure is from Liu and Ashegi [10]; symbols are experimental data referenced in [10]

TABLE I. IN-PLANE THERMAL CONDUCTIVITIES FOR SINGLE-CRYSTAL AND POLY-CRYSTAL SILICON FILMS AT 300K. THE RELAXATION TIME GIVEN IN SECOND COLUMN IS COMPUTED AS IN [11].

Material (Si)	Relaxation time (ps)	In-plane thermal conductivity (W/mK)	
		[10] (exp. data)	This work
Bulk	6.53	148	146
1 μ m-layer	6.42	140	139
B-doped ($10^{19} cm^{-3}$) 3 μ m-layer	6.22	130	135
poly-crystal 1 μ m-layer	1.65	13.1	15.4
B-doped ($1.6 \times 10^{19} cm^{-3}$) poly-crystal 3 μ m-layer	2.51	45.6	41.3

isotope, normal and Umklapp scattering processes. We thus show that at room temperature our model is in good agreement with both experimental data and the analytical model of Liu and Ashegi [10]. In [10], the thermal conductivity is calculated analytically with a relaxation time taking into account a geometrical factor and three polarization modes of phonons, which can explain the discrepancy with our work.

Table 1 presents computed thermal conductivities in some other materials at 300K. We have used the model developed in [11] to compute relaxation times depending on doping concentration and scattering on both grain and film diffusive boundaries. Without any fitting parameter and a constant size of silicon grains, we are in good agreement with the experimental data.

Besides, we have computed the cross-plane thermal conductivity in an amorphous SiO_2 film. We have used the equivalent formulation developed by Anderson and Freeman [12], leading to an equivalent mfp of is 0.58nm. This value leads to a relaxation time of 0.14ps. In a 50nm-thick film ($Kn \sim 0.01$), the LBM computed thermal conductivity is 1.385W/mK, in excellent agreement with the commonly measured value of 1.38W/mK [2]. As mentioned above, this result shows that the LBM is equivalent to FM in the diffusive regime and can be used instead of coupling with a Fourier solver to simulate heat transfers in SOI structures.

C. 2D SOI structure simulation

Finally, we have performed a 2D simulation of a SOI device shown in Figure 6. This structure has been taken from Narumanchi et al. [2] for comparison. Figure 6 shows the temperature contours at steady state. The peak temperature in

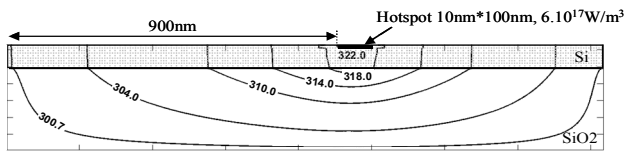


Figure 6 Steady state temperature profiles using a D2Q8 LBM (72nm-thick silicon layer on 243nm-thick SiO₂ layer, width of 1633nm, [2]).

the hotspot is 322K, to be compared to 326.4K in [2]. The difference can be explained by a slightly different specific heat and so for the local thermal conductivity.

IV. DISCUSSION OF D2Q24 LATTICE

Due to the discretization scheme D2Q8, we encounter some unphysical effects with our model in ballistic regime. This spatial propagation discretization anisotropy is emphasized by a too small relaxation rate inherent to ballistic transport.

We propose to increase the propagation directions number and we introduce a new lattice with 24 directions as shown on Figure 7. It can be considered as a projection of the 4-cells-radius circle on the mesh. The weights associated to each direction can not be derived with the same method as the D2Q8 lattice because this lattice is not fully isotropic (not invariant under the rotation group). Yet, the phonon gray model can be viewed as a diffusion hydrodynamic model, where such an isotropy is not necessary. Then we compute the weights according to symmetry and geometric angles. Figure 8 sums up the repartition of these weights at a normalized distance of 4 cells in inset. The resulting energy distribution with D2Q24 mimics rather well the exact isotropic repartition (straight line) of a point generation source compared to the D2Q8 result (dotted line), but this quality diminishes with the distance to the source point. The use of the D2Q24 in the LBM environment is our principal perspective.

V. CONCLUSION

In this work we have implemented a phonon transport model based on the Lattice Boltzmann scheme and on the “gray” model, using the OpenLB library. Boundary conditions take into account both specularly and thermal resistance. Complex 2D structures can be simulated thanks to the included treatment of interfaces. We have validated this model for steady state and transient temperature profiles; Computed

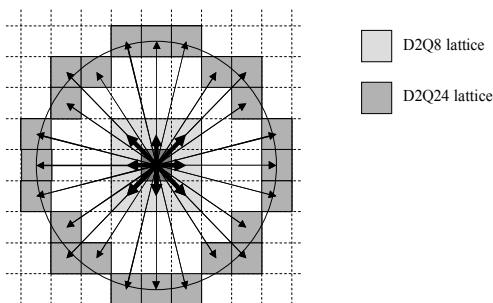


Figure 7 D2Q8 and D2Q24 lattices.

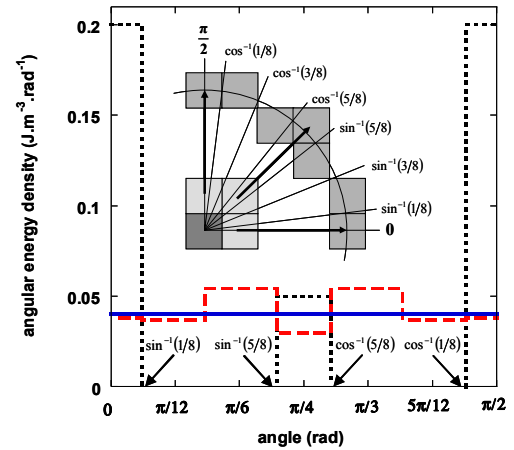


Figure 8 Angular energy density dispersion extracted in D2Q24 lattice (see Fig 2 and insert; bold arrows: D2Q8 sampling directions) from a punctual ballistic and isotropic phonon source; straight line: analytic solution, dotted-line: D2Q8 and dashed-line: D2Q24.

thermal conductivities at room temperature in various media are in good agreement with experiments. 2D simulation of a SOI structure is consistent with results in literature. We also propose a new lattice to go beyond the numerical limits of classical D2Q8 lattice in the ballistic case, i.e. to preserve isotropic propagation.

ACKNOWLEDGMENT

The authors would like to acknowledge N. Mingo from CEA-LITEN (Grenoble, France) and Jonas Lätt from Tufts Univ. (Boston, USA) for very helpful discussions.

REFERENCES

- [1] OpenLB, opensource C++ library, <http://www.openlb.org>.
- [2] S.V.J. Narumanchi, J.Y. Murthy and C.H. Amon, “Comparison of different phonon transport models for predicting heat conduction in SOI transistors”, JHT, vol 127, no 7, pp. 713-723, 2005.
- [3] J.M. Ziman, “Electrons and phonons”, Clarendon Press, 1960
- [4] S. Succi, “The lattice Boltzmann equation for fluid dynamics and beyond”, Oxford Univ. Press, 2001.
- [5] X. He, L.S. Luo; “Theory of the lattice Boltzmann method: from the Boltzmann equation to the lattice Boltzmann equation”, Phys. Rev. E, vol 56, no 6, pp. 6811-6817, 1997.
- [6] E.T. Swartz and R.O. Pohl, “Thermal boundary resistance”, Rev. Mod. Phys., vol 61, no 3, pp. 605-668, 1989.
- [7] R. Escobar, “Lattice Boltzmann modelling of phonon transport in silicon films”, PhD thesis, Carnegie Mellon Univ 2005.
- [8] J.Y. Murthy and C.H. Amon, “Computation of sub-micron thermal transport using an unstructured finite volume method”, JHT, vol 124, no 6, pp. 1176-1181, 2002.
- [9] M.G. Holland, “Analysis of lattice thermal conductivity”, Phys. Rev., vol 132, no 6, pp. 2461-2471, 1963.
- [10] W. Liu and M. Asheghi, “Phonon-boundary scattering in ultrathin single-crystal silicon layers”, APL, vol 84, no 19, pp. 3819-3821, 2004.
- [11] A.D. McConnell, S. Uma and K.E. Goodson, “Thermal conductivity of doped polysilicon layers”, J. MEMS, vol 10, no 3, pp. 360-369, 2001.
- [12] J.J. Freeman and A.C. Anderson, “Thermal conductivity of amorphous solids”, Phys. Rev. B, vol 34, no 8, pp. 5684-5690, 1986